

# Seismic behavior investigation of the steel multi-story moment frames with steel plate shear walls

Iman Mansouri<sup>1,2a</sup>, Ali Arabzadeh<sup>3b</sup>, Alireza Farzampour<sup>4c</sup> and Jong Wan Hu<sup>\*5,6</sup>

<sup>1</sup>Department of Civil Engineering, Birjand University of Technology, Birjand, Iran

<sup>2</sup>Institute of Research and Development, Duy Tan University, Da Nang 550000, Vietnam

<sup>3</sup>Department of Civil Engineering, Higher Education Complex of Hormozan, Birjand, Iran

<sup>4</sup>Department of Civil and Environmental Engineering, Virginia Tech, Blacksburg, United States

<sup>5</sup>Department of Civil and Environmental Engineering, Incheon National University, Incheon 22012, South Korea

<sup>6</sup>Incheon Disaster Prevention Research Center, Incheon National University, Incheon 22012, South Korea

(Received October 1, 2019, Revised September 24, 2020, Accepted September 26, 2020)

**Abstract.** Steel plate shear walls are recently used as efficient seismic lateral resisting systems. These lateral resistant structures are implemented to provide more strength, stiffness and ductility in limited space areas. In this study, the seismic behavior of the multi-story steel frames with steel plate shear walls are investigated for buildings with 4, 8, 12 and 16 stories using verified computational modeling platforms. Different number of steel moment bays with distinctive lengths are investigated to effectively determine the deflection amplification factor for low-rise and high-rise structures. Results showed that the dissipated energy in moment frames with steel plates are significantly related to the inside panel. It is shown that more than 50% of the dissipated energy under various ground motions is dissipated by the panel itself, and increasing the steel plate length leads to higher energy dissipation capability. The deflection amplification factor is studied in details for various verified parametric cases, and it is concluded that for a typical multi-story moment frame with steel plate shear walls, the amplification factor is 4.93 which is less than the recommended conservative values in the design codes. It is shown that the deflection amplification factor decreases if the height of the building increases, for which the frames with more than six stories would have less recommended deflection amplification factor. In addition, increasing the number of bays or decreasing the steel plate shear wall length leads to a reduction of the deflection amplification factor.

**Keywords:** steel plate shear wall; deflection amplification factor (cd); moment frame; multi-story buildings; hysteretic behavior

## 1. Introduction

Steel plate shear walls (SPSW) as lateral resisting systems are recently used for seismic resistance and fortification purposes. The steel plate shear walls are implemented in high-rise buildings due to high strength, initial stiffness, and ductility to limit the damages caused by external forces (Barua and Bhowmick 2019, Deng *et al.* 2019, Dhar and Bhowmick 2016, Kanvinde and Grilli 2012, Roberts and Ghomi 1991, Timler and Kulak 1983). Compared to concrete shear walls, these systems are able to reduce the total mass of the system while effectively use the space leading to less gravity forces transformed into the foundations, higher speed of construction and better quality control (Farzampour *et al.* 2015, Ghosh and Kharmale 2010, Ozcelik and Clayton 2017, Sabouri-Ghomi *et al.* 2012).

The steel plate shear walls are constructed based on the steel panels supported by beams and columns forming a

large cantilever system. Several studies determined that SPSW is an efficient and economical system especially for mid-rise and high-rise buildings, which effectively reduces the dead load and increase the unused floor space (Han *et al.* 2019, Ma *et al.* 2018, Pavir and Shekastehband 2017, Youssef *et al.* 2010). SPSWs are previously designed with thick infill plates or with stiffener to reduce the buckling occurrence possibilities; however, studies on the thin unstiffened SPSWs showed that the thin plates are able to reserve the strength with post-buckling characteristics leading to a desirable alternative system. The advantages of using thin plates are high initial stiffness, full hysteric behavior, ductility, and lightweight buildings compared to conventional systems (Farzampour *et al.* 2015, Qiu *et al.* 2018, Zhao *et al.* 2017). The SPSW systems are recently used in high rise buildings for reducing the seismic design and foundation load with more than 35% weight of the structure (Berman 2011, Youssef *et al.* 2010). However, large demand on the first and the upper most story of steel plate shear walls due to the tension field action is reported as an essential issue for high-rise buildings. The implementation of steel plate shear walls specifically limits the secondary structural damages in high-rise buildings (Driver *et al.* 1998). The major lateral resisting feature in steel plate shear walls is the post-buckling resistance, which allows out-of-plane deflections under relatively small shear

\*Corresponding author, Associate Professor  
E-mail: [jongp24@inu.ac.kr](mailto:jongp24@inu.ac.kr)

<sup>a</sup>Associate Professor

<sup>b</sup>Graduated Student

<sup>c</sup>Ph.D.

leading to developed tension field action resisting the shear loads (Berman *et al.* 2005, Elgaaly 1998).

Many studies are conducted to elaborate on the seismic behavior of the steel plate shear walls (Brando and De Matteis 2011, 2013, 2014, Curkovic *et al.* 2019, De Matteis *et al.* 2018, Farzampour and Yekrangnia 2014, Gholhaki and Ghadaksaz 2016, Liu *et al.* 2018, Paslar *et al.* 2020a, b, Phillips and Eatherton 2018, Qin *et al.* 2017, Qureshi and Bruneau 2019). According to the tension field theory, the multistory model is considered as a pin-ended tension only elements oriented diagonally for representing the tension field action. The angel of strip models is calculated initially based on the principle of the least work which is improved by considering bending strain energy (Berman and Bruneau 2003, Thorburn *et al.* 1983). The strip model is employed to analytically estimate the ultimate strength of the steel plate shear walls. Along the same lines, many design guidelines based on the plate frame interaction for analysis and design of shear walls are recently proposed to separately consider the plate, and the boundary element contribution in resistance of the structure (Farzampour *et al.* 2018a, b).

To understand the behavior of a system under earthquakes, nonlinear hysteretic response history analysis considering the nonlinear behavior of the beams and columns should be evaluated. However, the computational cost of nonlinear investigations and sensitiveness of the results to the selected ground motions makes the elastic structural analysis approach with lower seismic demand, a desirable approach for structural analysis. The elastic demand forces are typically reduced by reduction factor (R) based on the engineering judgment considering previous seismic behavior of the structures under harsh earthquakes (FEMA-P695 2009; FEMA-P1051 2015). The seismic deflections estimated under reduced demand forces, are typically less than the real deflection values; hence, deflection amplification factors ( $C_d$ ) are used to accordingly modify the deflections estimations based on the nonlinear behavior, which is schematically described in Fig. 1. It is noted that  $V_s$ ,  $V_y$  and  $V_e$  represent the design shear, yielding shear and elastic shear in Fig. 1.  $D_u$  and  $D_s$  are the ultimate story drift and design story drift.

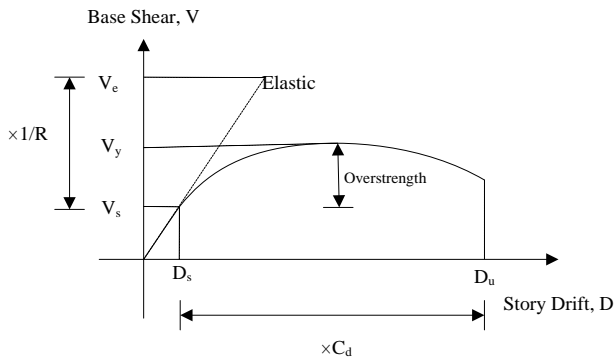


Fig. 1 The schematic representation of the deflection amplification factor ( $C_d$ ) and the reduction factor (R)

In this study, the amplification factors for the multi-story moment frame with steel plate shear walls are investigated. Steel moment frames with 4, 8, 12, and 16 stories and SPSW are investigated. In addition, the effect of story height, bay number, story number, SPSW span length are computationally investigated to derive amplification factor, energy dissipation capability of the components, and seismic deflections. In addition, static analysis and nonlinear dynamic analysis are subsequently conducted to evaluate the seismic behavior of the frames with steel plates.

## 2. Modeling methodology

The studied models are selected to cover various designed buildings with specific geometrical properties. The steel plate shear wall in all the models are located at the middle, and the sectional properties are designed with aid of the design software (ETABS). All the beams are designed with IPE sections and the infill plate thickness is varying from 3 mm to 6 mm. Subsequently, the linear static analysis and nonlinear response history analysis is conducted with OpenSees after modeling methodology verification study. The frames are designed with different story levels of 4,8, 12 and 16 stories with a constant story height of 3.1 m and the frame length of 3 m or 6 m simulating typical office buildings. The steel plate shear wall infill thickness is assumed to be varying from 3 mm up to 6 mm representing the typical values in SPSW application. The applied dead load and live loads are assumed to be 450 kg/m<sup>2</sup> and 200 kg/m<sup>2</sup>, respectively. The soil type is assumed to be type II and the base design acceleration is assumed to be 0.35g based on the BHRC design code [23]. It should be noted that the steel plate shear buckling angle for use in tension field action simulation is based on the reference (Thorburn *et al.* 1983) proposed equation represented in Eq. (1).

$$\tan^4 \alpha = \frac{\frac{2}{tL} + \frac{1}{A_c}}{\frac{2}{tL} + \frac{2h_s}{A_b L} + \frac{h_s^4}{180I_c L^2}} \quad (1)$$

in which  $t$ ,  $L$  and  $h_s$  are the thickness of the plate, length and the height of the story, respectively.  $A_c$ ,  $A_b$ , and  $I_c$  are the column cross-section, beam cross-section and column moment of inertia. Table 1 shows the studied models, the first letter number indicates the number of stories and the second number indicates the number of bays. It is noted that I, II, III, IV shown in Table 1 indicate the first four stories, second four stories, third four stories and fourth four stories of the building. For example, S4-36 indicates a steel moment with four stories and three bays in which the steel plate shear is located at the middle and designed based on the strip model theorem with infill plate length of 6 m, which is schematically shown in Fig. 2. The selected ground motions for nonlinear response history analysis are shown in Table 2 which are based on the Iranian Seismic Code of practice for the seismic-resistant design of buildings (BHRC 2014).

Table 1 The selected strip angles for steel plate shear wall design

| Name  | Strip Angle             | Strip NO | Selected Angle | Name   | Strip Angle | Strip NO | Selected Angle |
|-------|-------------------------|----------|----------------|--------|-------------|----------|----------------|
| S4-33 | All the stories<br>38.7 | 10       | 39.8           | S12-33 | I<br>37.6   | 10       | 39.8           |
| S4-36 | All the stories<br>41.3 | 9        | 40.6           | S12-36 | I<br>39.9   | 9        | 40.6           |
| S4-53 | All the stories<br>39.5 | 10       | 39.8           | S12-53 | I<br>37.5   | 10       | 39.8           |
| S4-56 | All the stories<br>41.3 | 9        | 40.6           | S12-56 | I<br>39.2   | 9        | 40.6           |
| S8-33 | I<br>39.5               | 10       | 39.8           | S16-33 | I<br>39.9   | 10       | 39.8           |
| S8-36 | I<br>41.1               | 9        | 40.6           | S16-36 | I<br>39.2   | 9        | 40.6           |
| S8-53 | I<br>39.0               | 10       | 39.8           | S16-53 | I<br>39.9   | 10       | 39.8           |
| S8-56 | I<br>40.1               | 9        | 40.6           | S16-56 | I<br>38.6   | 9        | 40.6           |

Table 2 Ground motion selected for nonlinear response history analysis

| No. | Earthquake |      |                 |         |
|-----|------------|------|-----------------|---------|
|     | Magnitude  | Year | Event           | PGA (g) |
| 1   | 7.1        | 1999 | Duzce, Turkey   | 0.739   |
| 2   | 7.6        | 1999 | Chi-Chi, Taiwan | 0.473   |
| 3   | 7.6        | 1999 | Chi-Chi, Taiwan | 0.398   |
| 4   | 7.5        | 1999 | Kocaeli, Turkey | 0.364   |
| 5   | 6.9        | 1995 | Kobe, Japan     | 0.225   |
| 6   | 6.9        | 1995 | Kobe, Japan     | 0.483   |
| 7   | 6.7        | 1994 | Northridge      | 0.471   |
| 8   | 6.7        | 1994 | Northridge      | 0.488   |
| 9   | 7.3        | 1992 | Landers         | 0.417   |
| 10  | 6.9        | 1989 | Loma Prieta     | 0.559   |
| 11  | 6.9        | 1989 | Loma Prieta     | 0.511   |
| 12  | 6.5        | 1979 | Imperial Valley | 0.366   |
| 13  | 6.5        | 1979 | Imperial Valley | 0.349   |

### 3. Verification of the modeling methodology

Steel plate shear wall test experiment conducted by Roberts and Sabouri-Ghomi (Roberts and Ghomi 1991) is investigated for capturing the hysteretic response under cyclic loading in which the infill plate is made of steel and aluminum. The boundary elements in this work are pinned and the panels are designed without stiffener. Fig. 3 shows the test experiment and the computational model for capturing the cyclic behavior. The panel ratio is equal to 1.0, and the plate thickness is equal to 0.83 mm for the steel material. In addition, Roberts and Sabouri-Ghomi reported

that the modulus of the elasticity is 2.02 GPA and yielding stress is 219 MPA for the studied steel plate shear wall (Roberts and Ghomi 1991). In the test specimen, two diagonally opposite pinned corners of the panel are connected to hydraulic grips which are considered in the computational model. The computational model is established by defining 30 elements working under compression simulating the strip model concept in OpenSees computational software. In order to computationally model the steel plate shear wall with

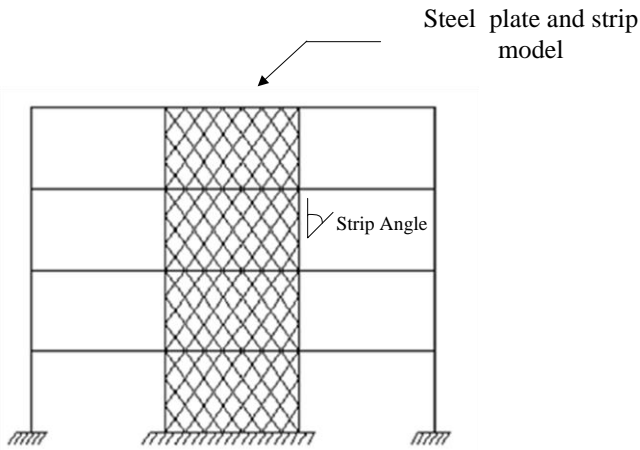
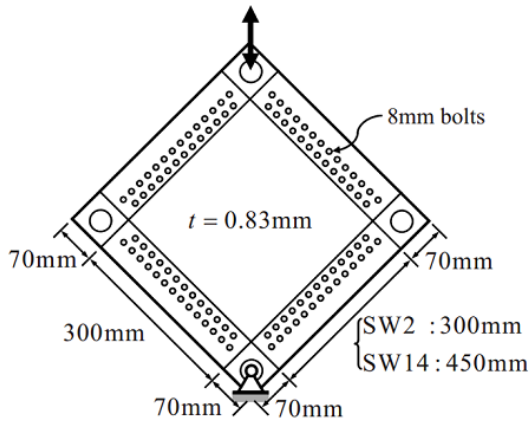
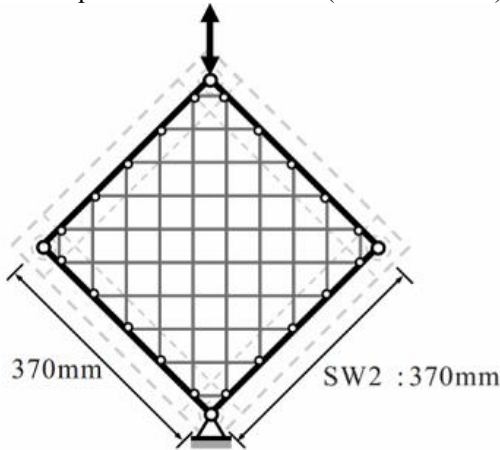


Fig. 2 The schematic representation of the model S4-36



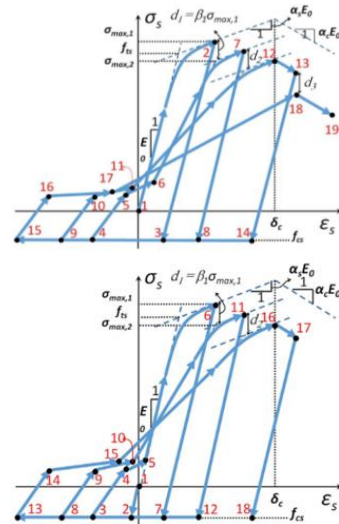
(a) The steel plate shear wall model (named as SW2)



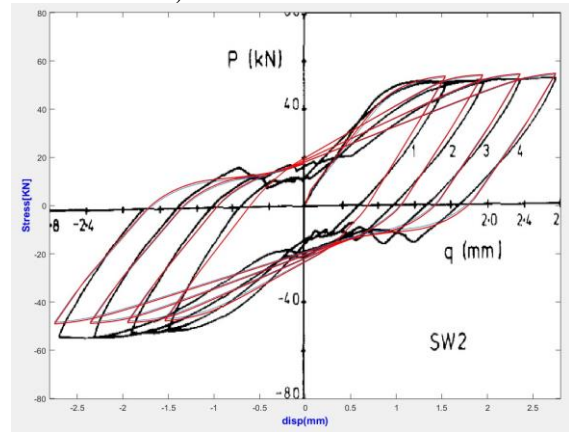
(b) The computational strip model

Fig. 3 Verification of modeling methodology with experimental test (Roberts and Ghomi 1991)

sufficient accuracy, the uniaxial material model proposed by Jalali and Banazadeh (2016) is used. The implemented material model considers the elastic modulus ( $E$ ), hardening ratio ( $b$ ), yielding stress ( $F_y$ ), plate thickness, plate height ( $H$ ), plate length ( $L$ ), which are schematically shown in 0.a.



(a) Choi-Park strip hysteric model (Jalali and Banazadeh 2016)



(b) Hysteretic behavior comparison of the experimental test and computational model

Fig. 4 Comparison between the predicted response in finite element verification study and experimental result of the Specimen SW2 (Roberts and Ghomi 1991)

To effectively capture the buckling branches of the laboratory test, Choi-Park strip force-deformation hysteric model is implemented based on the force-deformation of the shell elements represented in previous literature and showed in Fig. 4(a) (Jalali and Banazadeh 2016). The strips' tensional performance in re-loading after compressional buckling is considered, which is validated based on the proposed improvements for pinching cyclic rules. It is noted that recently-proposed Choi-Park force-displacement model considers the in-cycle and cyclic deterioration by introducing normalized cap strain and negative slope with respect to initial elastic modulus as compared to conventional strip model which is based on the computational cost-efficient macro-modeling techniques. Compared to conventional strip modeling methodology, the implemented modeling Choi-Park model assumes realistic rigid boundary action leading to precision in cyclic deterioration modes in larger displacements and accurate buckling prediction.

The deterioration and residual strength under cyclic loading condition are also considered to effectively capture the hysteretic behavior. The hysteretic behavior of this model is captured with the strip modeling theory, which is represented in Fig. 4(b). Results show that the computational model is able to capture the peak forces under cyclic loadings with the accuracy of more than 93%. In addition, the computational model was able to capture the hysteretic behavior in loading and unloading parts with more than 91% accuracy, which is shown in 0 Fig. 4(b).

**4. Discussion of results**

The Eigenvalue analysis is initially conducted for all the sixteen models developed for further computational investigations. The general trends indicate that by increasing the number of stories the natural period of the building increases and the model with the higher number of bays are stiffer than systems with the lower bay number. It is shown that the steel plate shear bay length is correlated with stiffening of the system in which the models with higher steel plate bay length have higher natural frequencies compared to the models with smaller bay length. Fig. 5 shows the natural periods of the verified models based on the number of stories, number of bays and bay length values.

The drifts of the moment frames with steel plate shear walls are calculated based on the nonlinear response history analysis. It is shown that the system with smaller shear wall span length has higher drift ratio due to the low stiffness. Higher number of moment frames would adversely affect the drift ratios, for which the steel plate shear effect on the total drifts are tangible especially in high-rise buildings.

Along the same lines, the deflection amplification factor for all the models is estimated based on the linear and nonlinear analysis shown in Fig. 1. From Figs. 6 and 7, it is concluded that for four-story buildings, increasing the number of bays and decreasing the SPSW bay length result in deflection amplification factor reduction. For eight-story structures, the highest amplification factors are related to the first stories, and it decreases if the number of bays increases or the SPSW bay length decreases. As it is shown in Fig. 7, there is 50% reduction in amplification factor values for eight-story buildings with SPSW compared to the corresponding four-story structure; however, for higher stories, the amplification factor values differences are less. It is noted that the amplification factor is reduced if the number of stories increases. In addition, it is shown that by increasing the height over length ratio of the SPSW, not only the amplification factor is reduced, but also the difference between the amplification factor of the higher stories with those of the lower stories are significantly reduced.

Based on the AISC 341, the amplification factor for steel plate shear walls with steel moment frames is reported to be 6.5. Story levels higher than sixth story in high rise buildings have generally less amplification factor than the prescribed values which shows the conservative proposed amplification factors by AISC standards for the structures

with six stories or more.

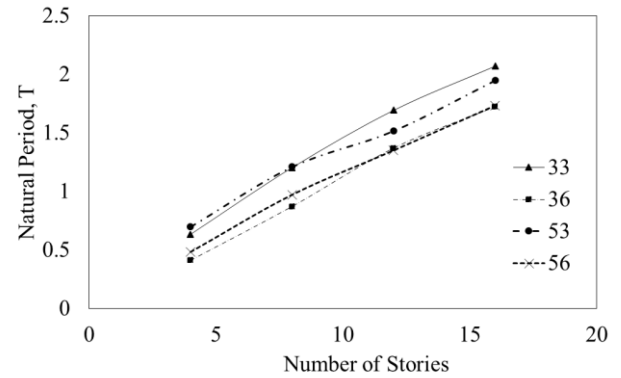


Fig. 5 Eigen Value analysis for evaluating the natural periods of the structures (For example, 33 means 3 bays with SPSW length of 3 m)

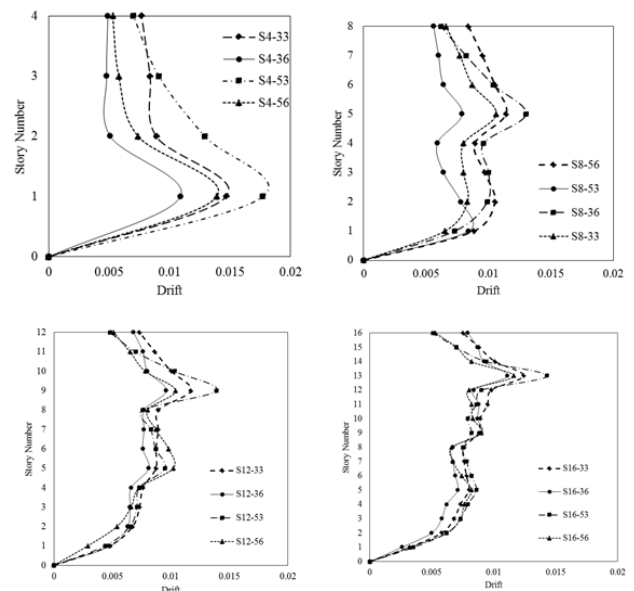


Fig. 6 The maximum drifts in structure

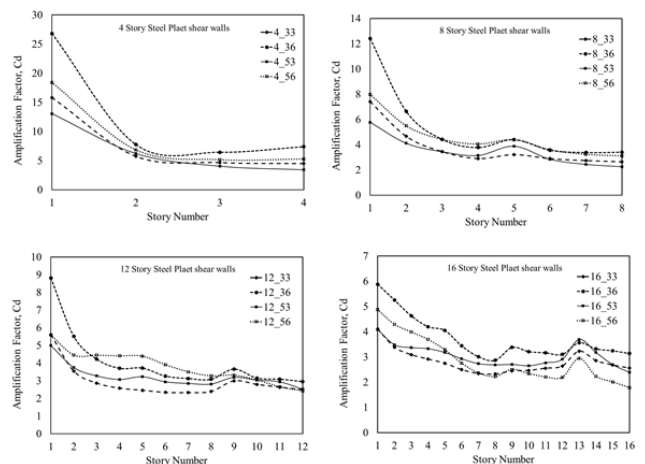


Fig. 7 Deflection amplification factor for multi-story buildings with steel moment frames and steel plate shear walls

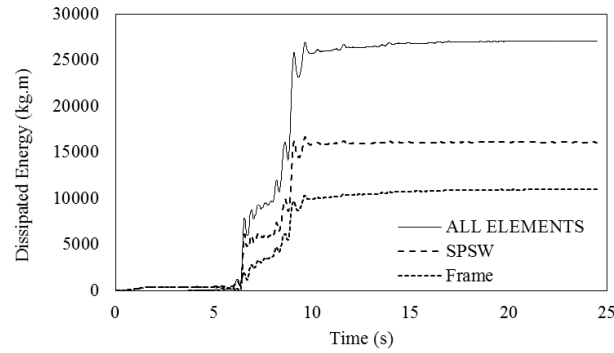


Fig. 8 Energy dissipation capability of S4-33 under Northridge earthquake

Table 3 Dissipated energy by different components in multi-story steel moment frame with SPSW

| Earthquake Number | Dissipated Normalized Energy |        |        |        |        |        |        |        |
|-------------------|------------------------------|--------|--------|--------|--------|--------|--------|--------|
|                   | Studied model                |        |        |        |        |        |        |        |
|                   | S12-33                       | S12-36 | S12-53 | S12-56 | S16-33 | S16-36 | S16-53 | S16-56 |
| 1                 | 0.46                         | 0.82   | 0.49   | 0.87   | 0.5    | 0.8    | 0.3    | 0.8    |
| 2                 | 0.76                         | 0.85   | 0.53   | 0.75   | 0.82   | 0.82   | 0.69   | 0.82   |
| 3                 | 0.13                         | 0.36   | 0.16   | 0.59   | 0.17   | 0.49   | 0.13   | 0.43   |
| 4                 | 0.11                         | 0.27   | 0.11   | 0.51   | 0.14   | 0.32   | 0.1    | 0.34   |
| 5                 | 0.24                         | 0.4    | 0.22   | 0.58   | 0.22   | 0.46   | 0.18   | 0.48   |
| 6                 | 0.6                          | 0.78   | 0.47   | 0.81   | 0.39   | 0.82   | 0.35   | 0.82   |
| 7                 | 0.53                         | 0.65   | 0.32   | 0.74   | 0.54   | 0.79   | 0.4    | 0.67   |
| 8                 | 0.36                         | 0.43   | 0.27   | 0.63   | 0.41   | 0.57   | 0.29   | 0.53   |
| 9                 | 0.49                         | 0.55   | 0.35   | 0.66   | 0.54   | 0.71   | 0.41   | 0.69   |
| 10                | 1                            | 0.96   | 0.85   | 0.95   | 0.99   | 0.97   | 0.97   | 0.96   |
| 11                | 0.45                         | 0.51   | 0.25   | 0.69   | 0.66   | 0.71   | 0.42   | 0.68   |
| 12                | 0.23                         | 0.49   | 0.22   | 0.73   | 0.23   | 0.44   | 0.17   | 0.49   |
| 13                | 0.24                         | 0.43   | 0.19   | 0.65   | 0.26   | 0.55   | 0.18   | 0.53   |
| Average           | 0.43                         | 0.58   | 0.34   | 0.71   | 0.45   | 0.65   | 0.35   | 0.63   |
| $\delta$          | 0.25                         | 0.21   | 0.19   | 0.12   | 0.25   | 0.18   | 0.24   | 0.18   |
| CV*               | 0.57                         | 0.36   | 0.57   | 0.17   | 0.55   | 0.28   | 0.67   | 0.28   |
| Average Total     | 0.51                         |        |        | 0.52   |        |        |        |        |

#### 4.1 Normalized dissipated energy

The dissipated energy is calculated for each of the steel plate shear wall models under all the ground motions. The normalized dissipated energy is calculated based on infill plates' normalized dissipated energy divided by the corresponding total energy dissipated by the steel plate shear wall. The steel plate shear wall and the moment frame contribute to the total dissipated energy of the structure. The effect of SPSW bay width, number of stories, and number of moment farms are investigated. Fig. 8 shows the energy dissipated by SPSW and the frame related to S4-33 model under Northridge earthquake. It is concluded that the structure with SPSW has approximately 130% increase in

the total dissipated energy compared to the structure built with steel moment frame only. Tables 3 and 4 show the contribution of SPSW in total energy dissipation capability of the system. It is shown that for buildings with 8, 12, and 16 stories SPSW were able to dissipate 56%, 51% and 52% of the total energy. In addition, the contribution of the steel plate shear walls in dissipating the energy caused by earthquakes are significant in low-and mid-rise buildings. The SPSW bay length increase, from 3 m to 6 m, increased the energy dissipation ratio of the steel plates by 25% on average, specifically for high-rise buildings. The number of steel moment frames has significant effect on the high-rise buildings energy dissipation capability especially for the systems with larger steel plate shear wall length.

Table 4 Dissipated energy by different components in multi-story steel moment frame with SP

| Earthquake Number | Dissipated Normalized Energy |       |       |       |       |       |       |       |
|-------------------|------------------------------|-------|-------|-------|-------|-------|-------|-------|
|                   | Studied model                |       |       |       |       |       |       |       |
|                   | S4-33                        | S4-36 | S4-53 | S4-56 | S8-33 | S8-36 | S8-53 | S8-56 |
| 1                 | 0.53                         | 0.53  | 0.57  | 0.63  | 0.68  | 0.63  | 0.61  | 0.69  |
| 2                 | 0.54                         | 0.54  | 0.7   | 0.51  | 0.88  | 0.79  | 0.81  | 0.82  |
| 3                 | 0.48                         | 0.48  | 0.46  | 0.55  | 0.35  | 0.42  | 0.37  | 0.44  |
| 4                 | 0.43                         | 0.43  | 0.45  | 0.51  | 0.31  | 0.39  | 0.32  | 0.41  |
| 5                 | 0.46                         | 0.46  | 0.47  | 0.51  | 0.38  | 0.39  | 0.4   | 0.46  |
| 6                 | 0.59                         | 0.59  | 0.63  | 0.6   | 0.85  | 0.74  | 0.66  | 0.83  |
| 7                 | 0.44                         | 0.44  | 0.5   | 0.51  | 0.51  | 0.42  | 0.46  | 0.54  |
| 8                 | 0.42                         | 0.42  | 0.49  | 0.53  | 0.31  | 0.43  | 0.36  | 0.42  |
| 9                 | 0.46                         | 0.46  | 0.53  | 0.52  | 0.4   | 0.57  | 0.39  | 0.58  |
| 10                | 0.71                         | 0.71  | 0.73  | 0.71  | 0.97  | 0.94  | 0.91  | 0.95  |
| 11                | 0.52                         | 0.52  | 0.55  | 0.59  | 0.44  | 0.59  | 0.4   | 0.53  |
| 12                | 0.75                         | 0.75  | 0.73  | 0.79  | 0.52  | 0.77  | 0.46  | 0.74  |
| 13                | 0.59                         | 0.59  | 0.56  | 0.66  | 0.44  | 0.56  | 0.41  | 0.54  |
| Average           | 0.53                         | 0.57  | 0.57  | 0.59  | 0.54  | 0.59  | 0.51  | 0.61  |
| $\delta$          | 0.10                         | 0.10  | 0.10  | 0.09  | 0.22  | 0.17  | 0.18  | 0.17  |
| CV*               | 0.19                         | 0.18  | 0.17  | 0.15  | 0.41  | 0.29  | 0.35  | 0.28  |
| Average Total     | 0.56                         |       |       |       | 0.56  |       |       |       |

## 5. Conclusions

The significant portion of the dissipated energy in moment frames with SPSW is related to the steel plate shear wall system. Results showed that more than 50% of the dissipated energy is conducted by SPSW, and by increasing the SPSW length, a larger portion of the energy is dissipated by the steel plate shear wall. The deflection amplification factor for multi-story buildings with steel moment frames and SPSW was 4.93 on average based on the nonlinear response analysis which is less than the conservative proposed values in standards. It is shown that the amplification factor decreases by increasing the height of the stories and a larger number of bays or larger SPSW bay length leads to reduction in deflection amplification factor. The contribution of the steel plate shear wall in dissipating the total energy caused by earthquakes is significant in low- and mid-rise buildings.

Based on the results of this study, the amplification factor for buildings with 4, 8, 12, and 16 are estimated to be 8.84, 4.26, 3.54, and 3.11, respectively. In addition, the highest amplification factors are generally related to lower stories which are sensitive to the bay length and the story height; therefore, it is recommended that different amplification factors to be used for frames with various geometrical conditions and story levels.

## Acknowledgments

This research was supported by a grant (20TBIP-C144315-03) from Technology Business Innovation Program (TBIP)

Program funded by Ministry of Land, Infrastructure and Transport of Korean government.

## References

- Barua, K. and Bhowmick, A.K. (2019), "Nonlinear seismic performance of code designed perforated steel plate shear walls", *Steel Compos. Struct.*, **31**(1), 85-98. <https://doi.org/10.12989/scs.2019.31.1.085>.
- Berman, J. and Bruneau, M. (2003), "Plastic analysis and design of steel plate shear walls", *J. Struct. Eng.*, **129**, 1448-1456. [https://doi.org/10.1061/\(ASCE\)0733-9445\(2003\)129:11\(1448\)](https://doi.org/10.1061/(ASCE)0733-9445(2003)129:11(1448)).
- Berman, J.W. (2011), "Seismic behavior of code designed steel plate shear walls", *Eng. Struct.*, **33**(1), 230-244. <https://doi.org/10.1016/j.engstruct.2010.10.015>.
- Berman, J.W., Celik, O.C. and Bruneau, M. (2005), "Comparing hysteretic behavior of light-gauge steel plate shear walls and braced frames", *Eng. Struct.*, **27**(3), 475-485. <https://doi.org/10.1016/j.engstruct.2004.11.007>.
- BHRC. (2014), Iranian code of practice for seismic resistant design of buildings: "standard 2800", Edition 4th. Iran (in Persian).
- Brando, G. and De Matteis, G. (2011), "Experimental and numerical analysis of a multi-stiffened pure aluminium shear panel", *Thin-Wall. Struct.*, **49**(10), 1277-1287. <https://doi.org/10.1016/j.tws.2011.05.007>.
- Brando, G. and De Matteis, G. (2013), "Buckling resistance of perforated steel angle members", *J. Constr. Steel Res.*, **81**, 52-61. <https://doi.org/10.1016/j.jcsr.2012.10.009>.
- Brando, G. and De Matteis, G. (2014), "Design of low strength-high hardening metal multi-stiffened shear plates", *Eng. Struct.*, **60**, 2-10. <https://doi.org/10.1016/j.engstruct.2013.12.005>.
- Curkovic, I., Skejic, D., Dzeba, I. and De Matteis, G. (2019), "Seismic performance of composite plate shear walls with

- variable column flexural stiffness”, *Steel Compos. Struct.*, **33**(1), 851-868. <https://doi.org/10.12989/scs.2019.33.1.851>.
- De Matteis, G., Brando, G., Caldosio, F. and D'Agostino, F. (2018), “Seismic performance of dual steel frames with dissipative metal shear panels”, *Ingegneria Sismica*, **35**(2), 124-141.
- Deng, E.F., Zong, L. and Ding, Y. (2019), “Numerical and analytical study on initial stiffness of corrugated steel plate shear walls in modular construction”, *Steel Compos. Struct.*, **32**(3), 347-359. <https://doi.org/10.12989/scs.2019.32.3.347>.
- Dhar, M.M. and Bhowmick, A.K. (2016), “Seismic response estimation of steel plate shear walls using nonlinear static methods”, *Steel Compos. Struct.*, **20**(4), 777-799. <https://doi.org/10.12989/scs.2016.20.4.777>.
- Driver, R.G., Kulak, G.L., Kennedy, D.J.L. and Elwi, A.E. (1998), “Cyclic test of four-story steel plate shear wall”, *J. Struct. Eng.*, **124**, 112-120.
- Elgaaly, M. (1998), “Thin steel plate shear walls behavior and analysis”, *Thin-Wall. Struct.*, **32**(1-3), 151-180. [https://doi.org/10.1016/S0263-8231\(98\)00031-7](https://doi.org/10.1016/S0263-8231(98)00031-7).
- Farzampour, A., Laman, J.A. and Mofid, M. (2015), “Behavior prediction of corrugated steel plate shear walls with openings”, *J. Constr. Steel Res.*, **114**, 258-268. <https://doi.org/10.1016/j.jcsr.2015.07.018>.
- Farzampour, A., Mansouri, I. and Hu, J.W. (2018a), “Seismic behavior investigation of the corrugated steel shear walls considering variations of corrugation geometrical characteristics”, *Int. J. Steel Struct.*, **18**(4), 1297-1305. <https://doi.org/10.1007/s13296-018-0121-z>.
- Farzampour, A., Mansouri, I., Lee, C.H., Sim, H.B. and Hu, J.W. (2018b), “Analysis and design recommendations for corrugated steel plate shear walls with a reduced beam section”, *Thin-Wall. Struct.*, **132**, 658-666. <https://doi.org/10.1016/j.tws.2018.09.026>.
- Farzampour, A. and Yekrangnia, M. (2014), “On the behavior of corrugated steel shear walls with and without openings”, *Proceedings of the 2nd European Conference on Earthquake Engineering and Seismology*, Turkey.
- FEMA-P695. (2009), Quantification of building seismic performance factors. Washington D.C.
- FEMA-P1051. (2015), NEHRP recommended seismic provisions: design examples. Washington D.C.
- Gholhaki, M. and Ghadaksaz, M.B. (2016), “Investigation of the link beam length of a coupled steel plate shear wall”, *Steel Compos. Struct.*, **20**(1), 107-125. <https://doi.org/10.12989/scs.2016.20.1.107>.
- Ghosh, S. and Kharmale, S.B. (2010), “Research on steel plate shear wall: Past, present and future, Structural Steel and Castings: Shapes and Standards, Properties and Applications”, Nova Science Publishers Inc.
- Han, Q., Zhang, Y., Wang, D. and Sakata, H. (2019), “Seismic behavior of buckling-restrained steel plate shear wall with assembled multi-RC panels”, *J. Constr. Steel Res.*, **157**, 397-413. <https://doi.org/10.1016/j.jcsr.2019.02.026>.
- Jalali, S.A. and Banazadeh, M. (2016), “Development of a new deteriorating hysteresis model for seismic collapse assessment of thin steel plate shear walls”, *Thin-Wall. Struct.*, **106**, 244-257. <https://doi.org/10.1016/j.tws.2016.05.008>.
- Kanvinde, A.M. and Grilli, D.A. (2012), *IBC SEAOC Structural/Seismic Design Manual Vol. 4, Examples for Steel-Frame Buildings*. Structural Engineers Association of California Sacramento, CA
- Liu, W.Y., Li, G.Q. and Jiang, J. (2018), “Capacity design of boundary elements of beam-connected buckling restrained steel plate shear wall”, *Steel Compos. Struct.*, **29**(2), 231-242. <https://doi.org/10.12989/scs.2018.29.2.231>.
- Ma, Z.Y., Hao, J.P. and Yu, H.S. (2018), “Shaking-table test of a novel buckling-restrained multi-stiffened low-yield-point steel plate shear wall”, *J. Constr. Steel Res.*, **145**, 128-136. <https://doi.org/10.1016/j.jcsr.2018.02.009>.
- Ozcelik, Y. and Clayton, P.M. (2017), “Strip model for steel plate shear walls with beam-connected web plates”, *Eng. Struct.*, **136**, 369-379. <https://doi.org/https://doi.org/10.1016/j.engstruct.2017.01.051>.
- Paslar, N., Farzampour, A. and Hatami, F. (2020a), “Infill plate interconnection effects on the structural behavior of steel plate shear walls”, *Thin-Wall. Struct.*, **149**. <https://doi.org/10.1016/j.tws.2020.106621>.
- Paslar, N., Farzampour, A. and Hatami, F. (2020b), “Investigation of the infill plate boundary condition effects on the overall performance of the steel plate shear walls with circular openings”, *Struct.*, **27**, 824-836. <https://doi.org/10.1016/j.istruc.2020.06.031>.
- Pavir, A. and Shekastehtband, B. (2017), “Hysteretic behavior of coupled steel plate shear walls”, *J. Constr. Steel Res.*, **133**, 19-35. <https://doi.org/10.1016/j.jcsr.2017.01.019>.
- Phillips, A.R. and Eatherton, M.R. (2018), “Large-scale experimental study of ring shaped-steel plate shear walls”, *J. Struct. Eng.*, **144**(8). [https://doi.org/10.1061/\(ASCE\)ST.1943-541X.0002119](https://doi.org/10.1061/(ASCE)ST.1943-541X.0002119).
- Qin, Y., Lu, J.Y., Huang, L.C.X. and Cao, S. (2017), “Flexural behavior of beams in steel plate shear walls”, *Steel Compos. Struct.*, **23**(4), 473-481. <https://doi.org/10.12989/scs.2017.23.4.473>.
- Qiu, J., Zhao, Q., Yu, C. and Li, Z. (2018), “Experimental studies on cyclic behavior of corrugated steel plate shear walls”, *J. Struct. Eng.*, **144**(11). [https://doi.org/10.1061/\(ASCE\)ST.1943-541X.0002165](https://doi.org/10.1061/(ASCE)ST.1943-541X.0002165).
- Qureshi, R.K. and Bruneau, M. (2019), “Behavior of steel plate shear walls subjected to repeated synthetic ground motions”, *J. Struct. Eng.*, **145**(4). [https://doi.org/10.1061/\(ASCE\)ST.1943-541X.0002281](https://doi.org/10.1061/(ASCE)ST.1943-541X.0002281).
- Roberts, T.M. and Ghomi, S.S. (1991), “Hysteretic characteristics of unstiffened plate shear panels”, *Thin-Walled Struct.*, **12**(2), 145-162. [https://doi.org/10.1016/0263-8231\(91\)90061-M](https://doi.org/10.1016/0263-8231(91)90061-M).
- Sabouri-Ghomi, S., Ahouri, E., Sajadi, R., Alavi, M., Roufegarinejad, A. and Bradford, M.A. (2012), “Stiffness and strength degradation of steel shear walls having an arbitrarily-located opening”, *J. Constr. Steel Res.*, **79**, 91-100. <https://doi.org/10.1016/j.jcsr.2012.07.017>.
- Thorburn, L.J., Kulak, G.L. and Montgomery, C.J. (1983), “Analysis of steel plate shear walls”, Structural Engineering Report 107, University of Alberta, Canada.
- Timler, P.A. and Kulak, G.L. (1983), “Experimental study of steel plate shear walls”, Structural Engineering, Report 114, University of Alberta, Canada.
- Youssef, N., Wilkerson, R., Fischer, K. and Tunick, D. (2010), “Seismic performance of a 55-storey steel plate shear wall”, *Struct. Des. Tall Spec. Build.*, **19**(1-2), 139-165. <https://doi.org/10.1002/tal.545>.
- Zhao, Q., Sun, J., Li, Y. and Li, Z. (2017), “Cyclic analyses of corrugated steel plate shear walls”, *Struct. Des. Tall Spec. Build.*, **26**(16). <https://doi.org/10.1002/tal.1351>.

BU